JOURNAL OF PROPULSION AND POWER
Vol. 18, No. 4, July–August 2002

Observations of Soot in the Combustion of Methanol/Toluene Spray Flames

C. T. Avedisian*
Cornell University, Ithaca, New York 14853-7501
C. Presser†
National Institute of Standards and Technology, Gaithersburg, Maryland 20899-8360
and
A. K. Gupta‡
University of Maryland, College Park, Maryland 20742

The influence of fuel chemical composition on flame structure and sooting trends in a swirling spray flame was investigated semiquantitatively using a light-scattering/dissymmetry ratio technique. Binary mixtures of toluene and methanol were examined under fixed aerodynamic and burner inlet flow conditions to show the effect of liquid composition. The sprays were generated using an air-assist atomizer. Methanol volume fractions ϕ of 0 (pure toluene), 0.25, 0.50, 0.75, 0.85, 0.90, 0.95, 0.99, and 1.0 (pure methanol) were examined. The results revealed little effect of methanol concentration on soot formation for $0.0 \le \phi \le 0.75$. However, for $\phi > 0.75$, the scattered light intensity decreased by almost four orders of magnitude, indicating a dramatic reduction in soot production above this concentration. Measurements of the dissymmetry ratio, complemented with Lorenz–Mie calculations of the scattering characteristics for a polydispersion of particles, indicated that no definite trends for the soot mean size were found with varying liquid composition within the resolution of the data. Direct light photography showed a hybrid flame structure for $\phi > 0.75$, which was blue and nonsooting near the atomizer exit, and yellow and luminous downstream, indicating preferential vaporization of methanol and a delay time for soot formation. The boundary between the yellow and blue zones of the flame moved toward the atomizer exit as the toluene concentration increased.

Nomenclature

C_{vv}	=	differential scattering cross section
$\bar{C}_{vv}$	=	mean scattering cross section
D	=	diameter
D_g	=	geometric mean diameter
D_{30}	=	volume mean diameter
f_v	=	volume fraction
k	=	imaginary part of the refractive index
m	=	refractive index
N	=	number density
n	=	real part of the refractive index
P	=	probability distribution function
Q_{vv}	=	absolute value of the vertical scattering coefficient
$\bar{Q}_{vv}$	=	measured scattered light intensity
R	=	dissymmetry ratio
r	=	radial position
S	=	swirl number
$\bar{S}$	=	system response function
x	=	size parameter
z	=	axial position
θ	=	scattering angle
λ	=	wavelength
σ_g	=	geometric mean standard deviation
ϕ	=	volume fraction

Received 25 June 1999; revision received 8 February 2002; accepted for publication 26 February 2002.

*Professor, Sibley School of Mechanical and Aerospace Engineering. Fellow AIAA.
†Group Leader, Process Measurements Division. Associate Fellow AIAA.
‡Professor, Department of Mechanical Engineering. Fellow AIAA.

I. Introduction

AROMATIC flames are highly luminous because of their propensity to soot, whereas alcohol flames are generally nonluminous and much less sooting.[1] This large difference in sooting tendency between these two classes of fuels suggests the possibility of controlling flame luminosity and particulate formation by mixing two fuels with large differences in their sooting tendencies with alcohol and aromatics representing extremes in this regard. On one hand, increased flame luminosity (that is, increased soot formation) with aromatic content can aid in identification and extinguishment of alcohol flames.[2,3] On the other, doping a highly sooting aromatic flame with an alcohol can reduce particulate formation and emission into the environment. This possibility has practical applications in the disposal of highly sooting liquid hazardous wastes, for example, chlorinated hydrocarbons, via spray-fired incineration.

This paper examines the influence of liquid chemical composition for methanol and toluene mixtures on soot formation in a spray flame. Measurements are made within the spray flame rather than far downstream or in the exhaust gas. Methanol volume fractions ϕ of 0 (pure toluene), 0.25, 0.50, 0.75, 0.85, 0.90, 0.95, 0.99, and 1.0 (pure methanol) were examined. Direct light photography was also used to record the generic features of the mixture spray flames. The methanol and toluene mixtures are completely miscible. To isolate the effect of composition, the operating conditions (that is, atomization air, combustion air, fuel and flow rates, swirl number, and atomizer type), were held constant for the range of flames investigated. Of the various types of atomizers,[4] pressure-jet and twin-fluid atomizers are most widely used. A twin-fluid (or air-assist) atomizer is used for this study because this atomizer design is widely used in spray-fired hazardous waste incinerators, which motivated the present study.

The extent of sooting and the variation of flame luminosity in methanol/toluene mixture flames have been noted in connection with liquid pool fires and wick flames.[2,3] No studies for sprays specifically related to the methanol/toluene system have been reported, although there is, in general, a dearth of quantitative

information on the sooting characteristics of spray flames. Beretta et al.[5,6] have carried out measurement of soot volume fraction in spray flames using a laser light scattering/extinction technique. The sprays were generated with a pressure-jet atomizer and several light industrial grade oils were examined. Although the fuels exhibited a range of sooting tendencies, the results did not emphasize or isolate the effects of additives on soot formation.

Related studies of individual isolated droplets have shown an effect of composition for methanol/toluene mixtures. An effect of methanol concentration on soot formation during combustion of methanol/toluene mixtures was observed in a study of a spherical droplet flame.[7] Soot that forms in a spherical droplet flame configuration is trapped between the droplet and flame in a 'shell' structure[8,9] that is concentric with the droplet and flame. From photographs of this special burning configuration, it was observed that toluene could burn without producing a visible soot shell by diluting the droplet with 75% (or higher) methanol (that is, volume fraction). Whereas single-droplet studies provide valuable insights into the behavior of a spray, the cumulative effects of droplet–droplet interactions coupled with gas-phase mixing in a system having a multitude of droplets of varying size and concentration (both spatially and temporally) makes direct extrapolation of burning single-droplet studies to spray flames difficult. It is, thus, necessary to carry out experiments directly on full sprays to best understand the influence of different parameters on soot formation.

In the present study, an ensemble light-scattering technique, based on measurement of the dissymmetry ratio, was used to obtain semiquantitative information of soot characteristics at various positions within methanol/toluene spray flames. A number of light-scattering techniques were considered to nonintrusively detect soot aggregates in spray flames. These include the light scattering/extinction ratio (SER),[6,10] laser-induced incandescence (LII),[11,12] and dissymmetry ratio (DR).[13–15] The SER method requires more flow symmetry than is present for the swirling, turbulent spray flames analyzed in the present study. The LII method has intriguing potential for full-field measurement of sooting tendencies in sprays and is a subject of ongoing research.

The DR technique was selected because it is reasonably simple to apply and can provide information at a spatially resolved location within the flowfield, regardless of the surrounding flow symmetry. It has good sensitivity for aggregates in the size range of 100–300 nm (Ref. 13). As a result, scattering from soot particles in this size range is used to assess the influence of composition on soot formation. Of course, measurement of the scattered light intensity (that is, scattering coefficient), by itself is insufficient to determine the amount of soot (that is, soot volume fraction). Such measurements must be supplemented by information on soot mean particle size. For the sprays examined in the present study, we will show that the scattered light intensity varies by many orders of magnitude compared to the small variation in mean particle size inferred from DR measurements. For this situation, scattered light intensity measurements do in fact alone give a measure of soot formation. In the analysis of the data, we assume the soot particles are spheres. Approaches have been discussed that correct for nonspherical aggregates.[16–18] Our goal here is to indicate semiquantitative trends in the tendency to soot with fuel composition for methanol/toluene spray flames, and the DR technique with the spherical aggregate assumption is adequate for this purpose.

II. Experimental Apparatus

Ensemble Light-Scattering Measurements

Information on soot formation was obtained using an ensemble light-scattering technique that was based on measurement of the DR. A schematic of the optical arrangement is shown in Fig. 1. The apparatus enables measurement of the particle scattering coefficient as a function of scattering angle and polarization of the incident and scattered light. The vertical scattering coefficient $Q_{vv}(\theta)$ is the power scattered in direction θ per unit solid angle, per unit volume, and per unit incident flux (per centimeter per steradian) for the vertically polarized incident and scattered light. The calculated dependence of

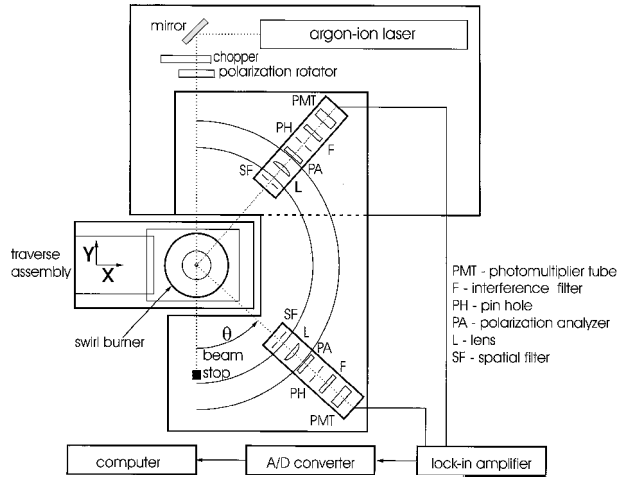

Fig. 1 Schematic of the optical arrangement used to measure the dissymmetry ratio.

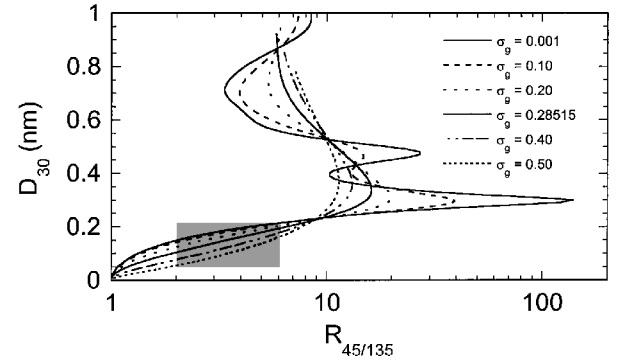

Fig. 2 Calculated variation of the particle volume mean diameter D_{30} with DR, $R_{45/135}$, based on Lorenz–Mie theory; shaded region identifies range of measurements.

DR on the particle mean diameter is then determined from Lorenz–Mie theory for a polydisperse system of droplets (Fig. 2). The DR, $R_{\theta 1/\theta 2}$, is defined as the ratio of the intensity scattered at two angles (θ_1, θ_2) symmetrical about 90 deg, that is, $\theta_1 = 180 \text{ deg} - \theta_2$ (Ref. 19):

$$R_{\theta_1/\theta_2}(\phi) = \frac{Q_{vv}(\theta_1, \phi)}{Q_{vv}(\theta_2, \phi)} \tag{1}$$

and

$$Q_{vv}(\theta_j, \phi) = \frac{\bar{Q}_{vv}(\theta_j, \phi)}{\bar{S}(\theta_j)} \tag{2}$$

where $\bar{Q}_{vv}(\theta_j, \phi)$ is the measured scattered light intensity (arbitrary units) that is corrected by the system response function $\bar{S}(\theta_j)$, to obtain an absolute value of the scattering coefficient $Q_{vv}(\theta_j, \phi)$. The subscript j represents the two scattering angles, $j = 1, 2$. To obtain $\bar{S}(\theta_j)$, calibration of the scattered light detection system is required to account for the effects of incident laser power, measurement probe volume, light collection efficiency, detector sensitivity, and electronic gain of the system. The calibration is carried out by introducing gases of known Rayleigh scattering cross section (that is, propane, butane, etc.) directly into the measurement volume.

The optical arrangement (Fig. 1) used a 4-W argon-ion laser as the light source that operated at the 514.5-nm laser line. The incident beam intensity was modulated with a mechanical chopper that operated at 1015 Hz. A polarization rotator sets the incident light polarization to the vertical orientation. Two similar light-detection systems were used to measure the scattered light intensity of the soot particles: one mounted at a scattering angle of $\theta = 45$ deg and the other positioned at $\theta = 135$ deg. (The scattering angles are measured from the forward scattering direction of propagation of the

laser beam.) Each detection system consisted of a polarization analyzer (positioned to obtain the vertical component of the scattered light), circular aperture that was placed in front of the optics to define the collection solid angle, collection lens, narrowband filter to reject background radiation, and a photomultiplier tube (PMT) detector. Both detection systems were mounted onto two concentric circular tracks to permit easy adjustment of the scattering angles.

A lock-in amplifier was used to reject background radiation and enhance the signal-to-noise ratio from the output signal of each PMT detector. An average of 2500 samples/reading were recorded by a microcomputer-baseddata acquisition system to ensure a better than 5% measurement repeatability at each position, with the lock-in amplifier set at a time constant of 0.03 Hz. Measurements were carried out at the stated positions in each flame several times and repeated for certain flames to ensure that the detected phenomena were indeed present.

Temporally resolved measurements of $Q_{vv}(\theta)$ were also carried out at $\theta = 105$ deg to check for the presence of liquid droplets in the pure methanol spray. This particular angle was chosen because the polarization ratio (that is, ratio of the horizontally to vertically polarized light), is sensitive to droplet Sauter mean diameter (see Ref. 20) though we did not actually determine the polarization ratio for the present study. Other angles could just as well have been selected for the purpose intended. A four-channel, 1-MHz, 12-bit data acquisition system was used to measure Q_{vv} on a temporal basis over a 120-s sampling period.

Combustion Facility

To determine the DR, $\bar{Q}_{vv}(\theta, \phi)$ is measured at two different scattering angles. The measurements are made in a spray combustion facility designed to simulate practical combustion systems.[21–24] The facility consists of a swirl burner with a movable 12-vane swirl cascade (Fig. 3); the vanes are rotated simultaneously to impart the desired degree of swirl intensity to the combustion airstream that surrounds the fuel atomizer. The nominal swirl number S was calculated from theory developed for a guide-vane cascade.[25] Experiments were carried out for swirling ($S = 0.53$) combustion airstreams under burning conditions.

A research air-assist atomizer was located along the centerline of the burner. Atomization air was supplied at a flow rate of 0.8 kg/h to atomize the low-pressure liquid fuel. A swirler located inside the atomization air passage (having a fixed vane angle of 60 deg) provided a nominal 60-deg hollow-cone spray. The fuel atomizer was operated at total air and fuel flow rates of 64.3 and 3.2 kg/h, respectively. The unconfined spray was injected vertically upward from the atomizer, located at the burner exit. A stepper-motor-driven, three-dimensional traversing arrangement was used to translate the burner assembly in the vertical and horizontal directions. All optical diagnostics were fixed in position about the burner assembly so that the burner translates independent of the optical equipment.

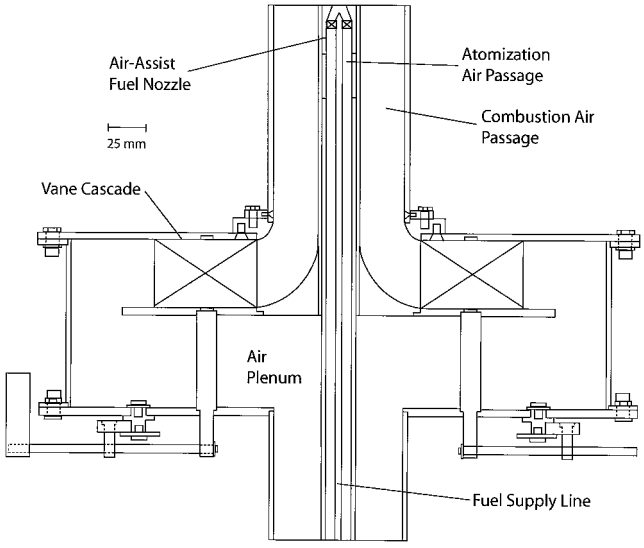

Fig. 3 Schematic of the movable-vane swirl burner.

A methanol spray flame was used to identify regions devoid of droplets. The vaporization rate of methanol is about the same as toluene based on a simple quasi-steady prediction using standard equations,[26] that is, methanol's higher heat of vaporization compared to toluene is offset by a lower product of gas density times mass diffusivity divided by liquid density for methanol compared to toluene.[27] When the aerodynamic conditions are kept fixed and it is noted that the thermophysical properties of the fuels used in this study do not have a strong effect on the overall hollow-cone spray structure for this air-assist atomizer,[4] regions devoid of methanol droplets will also be devoid of toluene droplets.

III. Lorenz–Mie Calculations

Calculations using Lorenz–Mie light-scattering theory (see Ref. 28) were carried out for a polydisperse system of droplets for interpretation of the light scattering data. For these calculations, a probability distribution function $P(D)$ is assumed, which is representative of the size distribution encountered in sprays. In this case, a two-parameter logarithmic normal distribution function is used, which is expressed as

$$P(D) = \frac{1}{\sqrt{2\pi}\sigma_g D} \exp\left(-\frac{[\ln(D/D_g)]^2}{2\sigma_g^2}\right) \tag{3}$$

where D is the soot particle diameter (micrometer), D_g is the geometric mean diameter (micrometer), and σ_g is the geometric mean standard deviation. The size distribution is normalized such that

$$\int P(D)\,\mathrm{d}D = 1$$

Based on the measured (that is, as obtained by means of various sampling techniques) or assumed particle size distribution, a mean particle size can be defined. In the following discussion, the volume mean diameter D_{30} is used to characterize the soot mean particle size,[10] and is defined as

$$D_{30} = \left[\int_0^\infty P(D) D^3\,\mathrm{d}D\right]^{\frac{1}{3}} \tag{4}$$

Note that the value of D_{30} is dependent on the assumed form of the distribution function.

The light scattered by an ensemble of spherical particles of varying size, at a given scattering angle θ, is determined from

$$Q_{vv}(\theta, \phi) = N(\phi)\bar{C}_{vv}(D_{30}, \sigma_g, \theta) \tag{5}$$

where N is the particle number density (per cubic centimeter) and $\bar{C}_{vv}$ is the mean scattering cross section (per square centimeter per steradian). This cross section is defined as

$$\bar{C}_{vv}(D_{30}, \sigma_g, \theta) = \int_0^\infty C_{vv}(\theta, x, m) P(D)\,\mathrm{d}D \tag{6}$$

where $x = \pi D/\lambda$ is the size parameter, $m = n - ik$ is the complex refractive index, λ is the wavelength of the incident light (micrometer), and C_{vv} is the differential scattering cross section for a specified particle size (per square centimeter per steradian). Also note that N is dependent on liquid composition ϕ (that is, the focus of this study) among other parameters.

The mean scattering cross section, $\bar{C}_{vv}$, is calculated from Lorenz–Mie theory, as a function of scattering angle, for prescribed values of m, σ_g, and D_g. From Eqs. (3) and (4), the volume mean diameter can then be expressed as[15]

$$D_{30} = D_g \exp\left(\tfrac{3}{2}\sigma_g^2\right) \tag{7}$$

The DR is then calculated, using the definition given in Eqs. (1) and (5), by

$$R_{\theta_1/\theta_2}(\phi) = \frac{\bar{C}_{vv}(D_{30}, \sigma_g, \theta_1)}{\bar{C}_{vv}(D_{30}, \sigma_g, \theta_2)} \tag{8}$$

It follows, therefore, that $R_{\theta 1/\theta 2}$ is independent of the particle number density. The measured values of $R_{\theta 1/\theta 2}$ from Eq. (1) can then be used to determine the particle mean size at any point in the spray from the calculated dependence of $R_{\theta 1/\theta 2}$ on D_{30}, that is, with Eqs. (7) and (8). Once the particle mean size is known, the particle volume fraction f_v can then be determined from the local measurements of Q_{vv} for one of the two scattering angles, and the calculated relationship of $\bar{C}_{vv}$ to D_{30}, that is, with Eqs. (6) and (7):[28]

$$f_v = (\pi/6)(Q_{vv}/\bar{C}_{vv})D_{30}^3 \tag{9}$$

Note that measurement of the DR does not require any calibration, whereas the Q_{vv} measurements do because the volume fraction is dependent on the absolute value of the scattering coefficient.

We choose $\theta_1 = 45$ deg and $\theta_2 = 135$ deg based on past work.[14,15] Figure 2 presents the calculated dependence of $R_{\theta 1/\theta 2}$ on D_{30} (using Eqs. (6) and (7)). The computations were carried out using the numerical code of Wiscombe.[29] For this study, m is assumed to be $1.90 - i0.55$ (Refs. 18 and 30), and the values of σ_g and D_g are unknown. Concerning σ_g, the computations were carried out for a range believed to be representative of a sooting flame, namely, 0.1, 0.2, 0.28515 (which approximates the self-preserving distribution,[15] solid line in Fig. 2), 0.4, and 0.5. For D_g, values were selected between 10 nm and 1 μm (in 10 nm increments). This range of D_g is inclusive of measurements for both small and large aggregates for flame-generated soot.[17] For each σ_g and D_g, the corresponding D_{30} was computed from Eq. (7), and DR was determined from Eqs. (6) and (8). As shown in Fig. 2, D_{30} is multivalued for certain ranges of $R_{45/135}$, for example, $2.2 < R_{45/135} < 130$ for $\sigma_g = 0.001$. This issue is overcome by selecting the range of mean particle diameters for a given σ_g from a reasonable expectation or direct sampling of the flame to measure soot aggregate size.

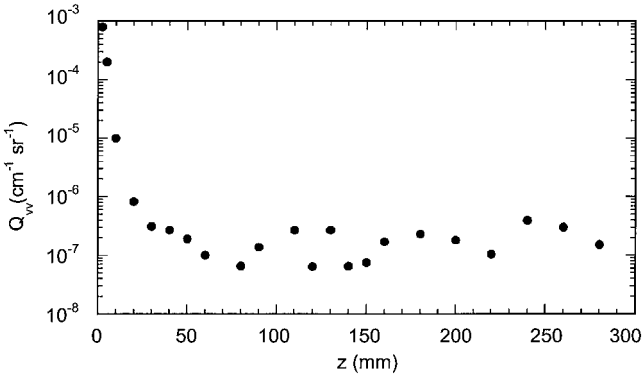

Fig. 4 Variation of the vertical scattering coefficient Q_{vv} with axial position z along the spray centerline at a scattering angle of 105 deg for a burning methanol spray.

IV. Results and Discussion

Because the air-assist atomizer used in the present study produces a hollow-cone spray, regions devoid of droplets will be along the centerline of the burner. Figure 4 shows the variation of Q_{vv} with z along the burner axis, that is, $r = 0$, for a burning methanol spray at a scattering angle of $\theta = 105$ deg. In Fig. 4, Q_{vv} decreases by four orders of magnitude in the range $0 < z < 50$ mm and thereafter remains in the range of 6×10^{-8} cm^{-1} sr^{-1} to 4×10^{-7} cm^{-1} sr^{-1}. This low signal strength for $z > 50$ mm is comparable to the scattering intensity of unpublished results for a propane flame. As already noted, toluene droplets are predicted to have the same vaporization rate as methanol, and thus, if there are no methanol droplets at a given location, toluene droplets will also not be present.

Figure 5 presents temporal sequences of the scattering intensity $\bar{Q}_{vv}$ at $\theta = 105$ deg for a nonburning methanol spray. Results are given for three different positions: along the spray boundary coincident with droplet trajectories (at $z = 10$ mm, $r = 8.9$ mm, Fig. 5a), along the centerline (at $z = 10$ mm, $r = 0$, Fig. 5b), and again along the centerline but farther downstream (at $z = 100$ mm, $r = 0$, Fig. 5c). A 20-s interval of the total acquisition time for each position is presented in Fig 5. Each data point in Fig. 5 signifies the total light scattered from an ensemble of particles present in the measurement volume during the microsecond data acquisition time. The relative infrequency of the signals (indicative of the presence of droplets) along the centerline at $z = 10$ mm and $z = 100$ mm indicates that few, if any, droplets are present in this case where droplet vaporization is negligible (as compared to the burning case). Again, the overall hollow-cone structure of the spray will be similar regardless of the fuel because the atomizer type controls the spray

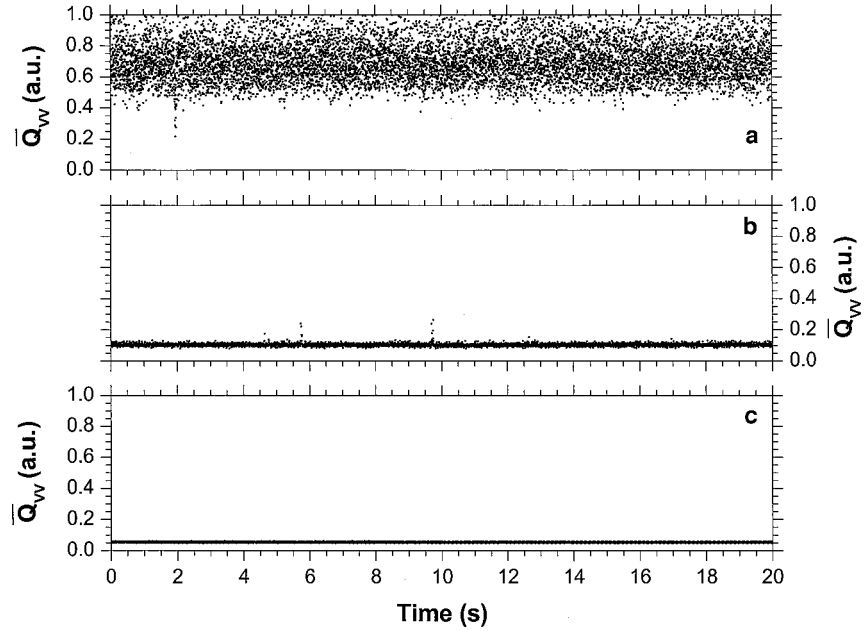

Fig. 5 Time-resolved measurements of $\bar{Q}_{vv}$ (arbitrary units) over a 20-s interval for a nonburning methanol spray at a) $z = 10$ mm and $r = 8.9$ mm, b) $z = 10$ mm and $r = 0$, and c) $z = 100$ mm and $r = 0$.

structure. As a result of these findings, axial positions of 102 and 152 mm along the burner centerline were chosen to carry out DR measurements for the methanol/toluene mixture flames. These positions are sufficiently downstream of the atomizer that droplets should not be present.

The variation of Q_{vv} with methanol composition is presented in Fig. 6 at $z = 102$ mm (Fig. 6a) and 152 mm (Fig. 6b) for $\theta = 45$ and 135 deg. The scattered light intensity is relatively insensitive to concentration over the range $0 \leq \phi \leq 0.75$, whereas it decreases by four orders of magnitude from $\phi = 0.75$ to $\phi = 1.0$. Because of this large reduction in signal with increasing methanol dilution, more

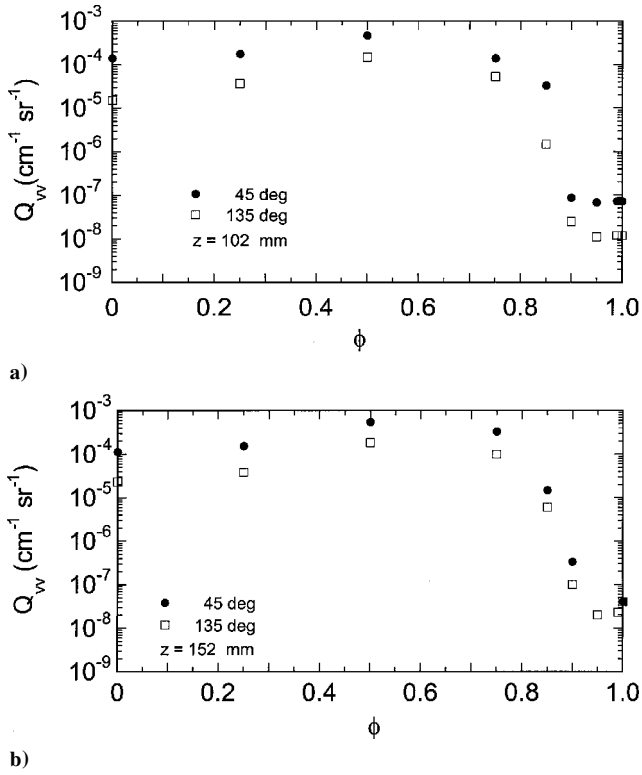

Fig. 6 Variation of the vertical scattering coefficient Q_{vv} with methanol volume fraction along the burner centerline for scattering angles of 45 and 135 deg for a) $z = 102$ mm and b) $z = 152$ mm.

compositions were examined at higher methanol loadings (that is, volume fractions of 0.85, 0.9, 0.95, 0.99, and 1.0) to show the trend better. The large decrease in the value of Q_{vv} for $\phi > 0.75$ is also close to the composition where soot oxidation extends over the entire plume of the flame, as will be shown by color photographs of these flames. However, we cannot relate Q_{vv} to the amount of soot (in the sense of the soot volume fraction) until we know more about how D_{30} varies with composition. This point will also be addressed.

Figure 7 is a series of color photographs of the flame structure for four of the methanol/toluene spray flames investigated in this study. The laser beam (horizontal green line) that is visible in Figs. 7a and 7b is positioned at $z = 102$ mm. For volume fraction greater than 50% toluene, the spray flame structure is essentially unchanged from Fig. 7d. The highly nonsymmetric nature of the spray is evident. The nonluminous blue color for the pure methanol flame (Fig. 7a) signifies a nonsooting spray flame. With 10% toluene (Fig. 7b), a hybrid flame structure exists in which the region near the atomizer is blue and nonsooting, and the downstream portion of the plume is yellow from the lack of soot oxidation. The dotted line marks qualitatively the boundary between the upstream nonsooting and the downstream sooting zone. This hybrid structure may be attributed to three effects: 1) preferential vaporization in which methanol dominates evaporation early followed by toluene evaporation with its highly sooting nature; 2) a delay in soot formation after ignition, which is a natural byproduct of any droplet and spray burning process; and 3) strong convection, which spreads out the boundary between the upstream nonluminous (blue) and downstream luminous (yellow) zones. Methanol will vaporize first in a methanol/toluene mixture because its boiling point is lower than toluene, that is, 337 K for methanol and 383 K for toluene (Ref. 31). As more toluene is added to the mixture, methanol is depleted sooner during combustion, and the blue zone boundary is reduced in size near the atomizer exit. At higher toluene loadings, for example 25% toluene, (Fig. 7c), the blue zone disappears altogether as toluene dominates the vaporization process throughout.

A hybrid spray flame structure has also been observed for single-component spray flames,[21] binary mixtures of methanol/dodecanol spray flames,[22,32] and spherical droplet flames.[7] Single-component sprays sometimes have a blue upstream region and a yellow downstream zone that is attributed to the delay in soot formation after ignition. Spherical droplet flames of methanol and toluene mixtures[8] have also shown a tendency to be influenced by mixture composition, namely, the soot shell around the droplet disappears for methanol volume fractions above 0.75.

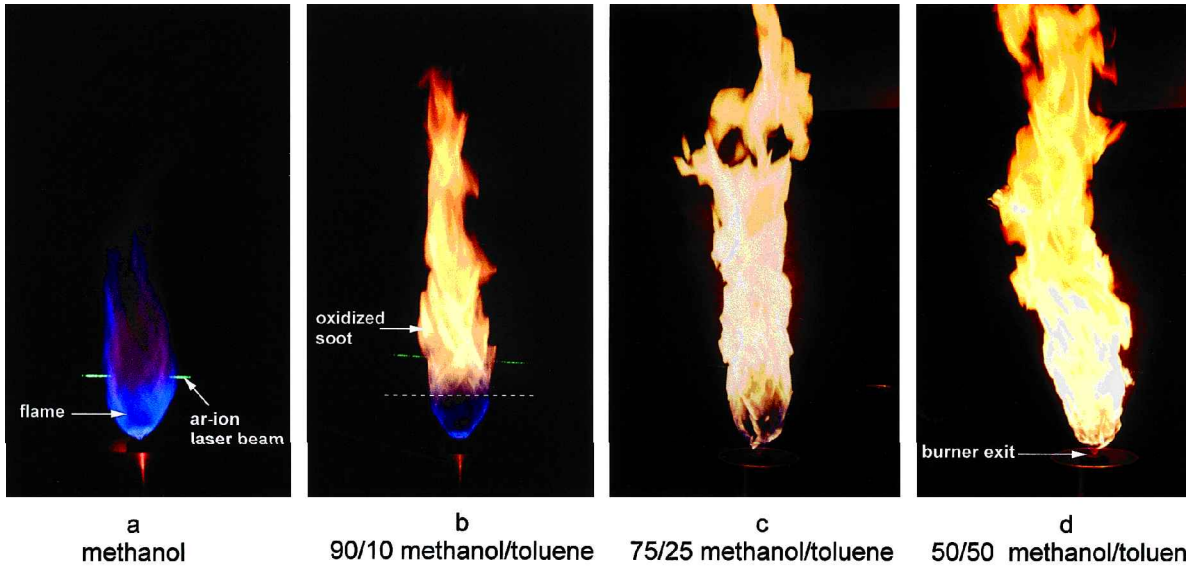

Fig. 7 Influence of mixture composition on flame structure and tendency to soot for volume fractions: a) 100% (pure methanol), b) 90/10% methanol/toluene where dotted line marks the boundary between the upstream nonsooting zone and downstream sooting zone, c) 75/25% methanol/toluene, and d) 50/50% methanol/toluene. Laser beam for the scattering measurements visible in Figs. 7a and 7b.

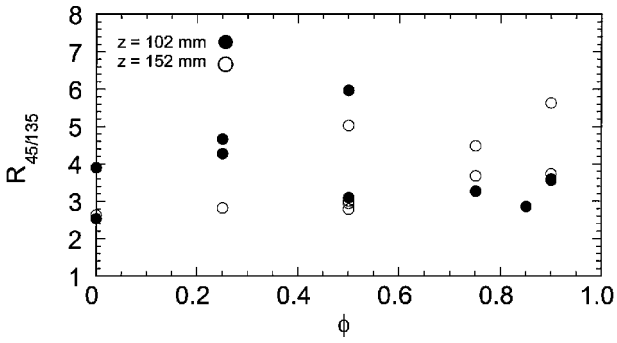

Fig. 8 Variation of DR $R_{45/135}$ with methanol volume fraction for $z = 102$ and 152 mm, along the burner centerline; shaded region of Fig. 2 indicates range of D_{30} expected from these values of $R_{45/135}$.

Figure 8 presents the variation of the DR with mixture composition at two downstream positions along the spray centerline. Results are not given for $\phi \geq 0.9$ because of the low signal levels at these higher methanol mixture fractions. The combustion gases will scatter light in the Rayleigh limit as $\phi \to 1$, corresponding to methanol (which is nonsooting under atmospheric conditions) and, thus, $R_{45/135} \to 1$. As indicated in Fig. 8, there is no clear trend, that is, $R_{45/135}$ does not have a clear dependency with ϕ. The DR ranges from 2 to 6 with mean values of $R_{45/135} = 3.79$ for $z = 102$ mm and $R_{45/135} = 3.66$ for $z = 152$ mm.

To determine the volume mean diameter, it is necessary to determine which curve (that is, value of σ_g) to use in Fig. 2. Unfortunately, not enough information is available from the measurements to determine σ_g. Also, the curves in Fig. 2 become multivalued with increasing values of $R_{45/135}$, and, thus, one must identify a portion of the selected curve that is relevant to the particle size range (that is, D_{30}) of interest. As noted above, the values of $R_{45/135}$ varied from 2 to 6. Köylü et al.[17] state that soot aggregate size varies from about 10 nm at the start of soot formation to about 1 μm for large buoyant turbulent diffusion flames. Therefore, it is reasonable to assume that the soot aggregate sizes detected in this study within the flame will generally be under 500 nm. The shaded region in Fig. 2 indicates the range of volume mean diameters, which is reasonable to expect. The results in Fig. 8 indicate that since $2 < R_{45/135} < 6$, one obtains $55 < D_{30} < 213$ nm from Fig. 2, which is a reasonable mean size range for soot aggregates. For this range of mean diameters, D_{30}^3 changes by a factor of 58, whereas Fig. 6 indicates that Q_{vv} changes by four orders of magnitude over the range of $0 < \phi < 1$. As a result, the dominant factor influencing f_v [see Eq. (9)] is Q_{vv}, and thus, variation of soot formation tracks with Q_{vv} for the methanol/toluene mixture flames examined in this study.

V. Summary

The influence of liquid composition on soot formation in methanol/toluene spray flames was investigated using a light-scattering/dissymmetry ratio technique and direct light photography. The light-scattering measurements were carried out at selected positions in the spray flames devoid of droplets.

The results indicated no systematic variation of aggregate volume mean diameter with methanol volume fraction in the range of liquid compositions that the DR could detect particles. The vertical scattering coefficient, however, decreased by almost four orders of magnitude for $\phi > 0.75$, indicating a strong reduction in soot formation. These results suggest the existence of a range of methanol/toluene mixtures over which the sooting tendency is strongly influenced by liquid composition. A hybrid flame structure, consisting of a blue transparent zone near the atomizer followed by a yellow luminous zone downstream, was attributed to preferential vaporization of the mixture droplets.

Acknowledgments

Early financial support from the New York State Center for Hazardous Waste Management is acknowledged. The authors benefited from helpful discussions with Joseph Hodges of the National Institute of Standards and Technology.

References

[1]Glassman, I., "Soot Formation in Combustion Processes," *Proceedings of the Twenty-Second International Symposium on Combustion*, Combustion Inst., Pittsburgh, PA, 1988, pp. 295–311.

[2]Anderson, J. E., Magyari, M. W., and Siegl, W. O., "Concerning the Luminosity of Methanol–Hydrocarbon Diffusion Flames," *Combustion Science and Technology*, Vol. 43, No. 3–4, 1985, pp. 115–125.

[3]Sorek, H., and Anderson, J. E., "^{14}C Study of Relative Fuel-to-Soot Carbon Conversion in Premixed Flames," *Combustion Science and Technology*, Vol. 49, No. 3–4, 1986, pp. 201–204.

[4]Lefebvre, A. H., *Atomization and Sprays*, Hemisphere, New York, 1989, pp. 273, 274.

[5]Beretta, F., Cavaliere, A., Ciajolo, A., D'Alessio, A., Langella, C., and DiLorenzo, A., "Laser Light Scattering, Emission/Extinction Spectroscopy and Thermogravimetric Analysis in the Study of Soot Behaviour in Oil Spray Flames," *Proceedings of the Eighteenth International Symposium on Combustion*, Combustion Inst., Pittsburgh, PA, 1981, pp. 1091–1096.

[6]Beretta, F., D'Alessio, A., and Noviello, C., "Spray Vaporization and Soot Formation in Flames Generated by Light Oils with Different Chemical Composition," *Proceedings of the Twenty-First International Symposium on Combustion*, Combustion Inst., Pittsburgh, PA, 1986, pp. 1133–1140.

[7]Jackson, G. S., Avedisian, C. T., and Yang, J. C., "Soot Formation During Combustion of Unsupported Methanol/Toluene Mixture Droplets in Microgravity," *Proceedings of the Royal Society of London, Series A: Mathematical and Physical Sciences*, Vol. 435, No. 1894, 1991, pp. 359–369.

[8]Avedisian, C. T., "Soot Formation in Spherically Symmetric Droplet Combustion," *Physical and Chemical Aspects of Combustion*, Gordon and Breach, Amsterdam, Netherlands, 1997, pp. 135–160.

[9]Avedisian, C. T., "Recent Advances in Soot Formation from Spherical Droplet Flames at Atmospheric Pressure," *Journal of Propulsion and Power*, Vol. 16, No. 4, 2000, pp. 628–635.

[10]Santoro, R. J., Semerjian, H. G., and Dobbins, R. A., "Soot Particle Measurements in Diffusion Flames," *Combustion and Flame*, Vol. 51, No. 2, 1983, pp. 203–218.

[11]Gupta, S. B., Ni, I., and Santoro, R. J., "Spatial and Time Resolved Soot Volume Fraction Measurements in Methanol/Benzene Droplet Flames," Chemical and Physical Processes in Combustion, Clearwater Beach, FL, *Proceeding of the Fall Technical Meeting, Eastern States Section of the Combustion Institute*, 1994, pp. 238–241.

[12]Vander Wal, R. L., Jensen, K. A., and Choi, M. Y., "Simultaneous Laser-Induced Emission of Soot and Polycyclic Aromatic Hydrocarbons Within a Gas-Jet Diffusion Flame," *Combustion and Flame*, Vol. 109, No. 3, 1997, pp. 399–414.

[13]Zachariah, M. R., Chin, D., Semerjian, H. G., and Katz, J. L., "Dynamic Light Scattering and Angular Dissymmetry for the In Situ Measurement of Silicon Dioxide Particle Synthesis in Flames," *Applied Optics*, Vol. 28, No. 3, 1989, pp. 530–536.

[14]Zachariah, M. R., Chin, D., Semerjian, H. G., and Katz, J. L., "Silica Particle Synthesis in a Counterflow Diffusion Flame Reactor," *Combustion and Flame*, Vol. 78, No. 1–2, 1989, pp. 287–298.

[15]Dobbins, R. A., Santoro, R. J., and Semerjian, H. G., "Interpretation of Optical Measurements of Soot in Flames," Combustion Diagnostics by Nonintrusive Methods, edited by T. D. McCay and J. A. Roux, Progress in Astronautics and Aeronautics, Vol. 92, 1984, AIAA, New York, pp. 208–237.

[16]Dobbins, R. A., and Megaridis, C. M., "Absorption and Scattering of Light by Polydisperse Aggregates," *Applied Optics*, Vol. 30, No. 33, 1991, pp. 4747–4754.

[17]Köylü, Ü. Ö., Faeth, G. M., Farias, T. L., and Carvalho, M. G., "Fractal and Projected Structure Properties of Soot Aggregates," *Combustion and Flame*, Vol. 100, No. 4, 1995, pp. 621–633.

[18]Puri, R., Richardson, T. F., Santoro, R. J., and Dobbins, R. A., "Aerosol Dynamics Processes of Soot Aggregates in a Laminar Ethene Diffusion Flame," *Combustion and Flame,* Vol. 92, No. 3, 1993, pp. 320–333.

[19]Kerker, M., *The Scattering of Light and Other Electromagnetic Radiation*, Academic Press, New York, 1969, p. 432.

[20]Bohren, C. F., and Huffman, D. R., *Absorption and Scattering of Light by Small Particles*, Wiley, New York, 1983, pp. 99–116.

[21]Presser, C., Gupta, A. K., Avedisian, C. T., and Semerjian, H. G., "Fuel Property Effects on the Structure of Spray Flames," *Proceedings of the Twenty-Third International Symposium on Combustion*, Combustion Inst., Pittsburgh, PA, 1990, pp. 1361–1367.

[22]Presser, C., Gupta, A. K., Avedisian, C. T., and Semerjian, H. G., "Effect of Dodecanol Content on the Combustion of Methanol Spray Flames," *Atomization and Sprays*, Vol. 4, No. 2, 1994, pp. 207–222.

[23]Presser, C., Gupta, A. K., Semerjian, H. G., and Avedisian, C. T., "Droplet Transport in a Swirl-Stabilized Spray Flame," *Journal of Propulsion and Power*, Vol. 10, No. 5, 1994, pp. 631–638.

[24]Gupta, A. K., Presser, C., Hodges, J. T., and Avedisian, C. T., "Role of Combustion on Droplet Transport in Pressure-Atomized Spray Flames," *Journal of Propulsion and Power*, Vol. 12, No. 3, 1996, pp. 543–553.

[25]Beér, J. M., and Chigier, N. A., *Combustion Aerodynamics*, Wiley, New York, 1972, pp. 109–112.

[26]Glassman, I., *Combustion*, 2nd ed., Academic Press, London, 1987, pp. 265–267.

[27]Reid, R. C., Prausnitz, J. M., and Poling, B. E., *The Properties of Gases and Liquids*, 4th ed., McGraw–Hill, New York, 1987, Chaps. 3, 11, pp. 670–703.

[28]Dobbins, R. A., Crocco, L., and Glassman, I., "Measurement of Mean Particle Sizes of Sprays from Diffractively Scattered Light," *AIAA Journal*, Vol. 1, No. 8, 1963, pp. 1882–1886.

[29]Wiscombe, W. J., "Mie Scattering Calculations: Advances in Technique and Fast, Vector-Speed Computer Codes," National Center for Atmospheric Research, NCAR/TN-140 + STR, Boulder, CO, June 1979.

[30]Lee, S., and Tien, C. L., "Optical Constants of Soot in Hydrocarbon Flames," *Proceedings of the Eighteenth International Symposium on Combustion*, Combustion Inst., Pittsburgh, PA, 1981, pp. 1159–1166.

[31]Reed, R. J., *North American Combustion Handbook*, Vol. 2, North American, Cleveland, OH, 1997, pp. 284–288.

[32]Presser, C., Gupta, A. K., Avedisian, C. T., and Semerjian, H. G., "Combustion of Methanol and Methanol/Dodecanol Spray Flames," *Journal of Propulsion and Power*, Vol. 8, No. 3, 1992, pp. 553–559.